Optik 122 (2011) 1179–1182

Contents lists available at ScienceDirect

Optik

journal homepage: www.elsevier.de/ijleo

Defect structure and nonvolatile hologram storage properties in Hf:Fe:Mn:$LiNbO_3$ crystals

Zifan Zhou [a,b], Biao Wang [a,*], Shaopeng Lin [a], Yilun Li [a], Kun Wang [a]

[a] School Phys Science & Engineering, Sun Yat-Sen University, Guangzhou 510275, China
[b] College of Science, Foshan University, Foshan 528000, China

ARTICLE INFO

Article history:
Received 24 January 2010
Accepted 22 July 2010

Keywords:
Hf:Fe:Mn:$LiNbO_3$
Optical damage resistance
Holographic recording
Two-photon fixed method

ABSTRACT

A series of Hf:Fe:Mn:$LiNbO_3$ crystals with various levels of HfO_2 doping were grown by Czochralski technique. The infrared spectra and ultraviolet spectra were measured and discussed to investigate their structure and defects. The optical damage resistance was characterized by the transmitted beam pattern distortion method. The nonvolatile two-color holographic recording experimental results showed that the recording speed was faster with the increase of HfO_2 doping concentration and at the same time little loss of nonvolatile diffraction efficiencies could be achieved.

1. Introduction

Lithium niobate ($LiNbO_3$) crystal is one of the most widely used photorefractive materials in the holographic volume storage [1,2]. A key problem in holographic storage using photorefractive $LiNbO_3$ crystals is the volatility. The phase grating is easily erased by the readout light of symmetrical intensity. An effective technique was developed to realize nonvolatile recording in $LiNbO_3$ crystals doped with shallower iron centers ($Fe^{2+/3+}$) and deeper manganese centers ($Mn^{2+/3+}$) [3,4]. But its applications in holographic memory devices are severely limited by optical damage [5]. Doping with damage-resistant addictives is found to be an effective method to increase the optical damage resistance [6]. Some damage-resistant elements, such as Zn [7], Mg [8], In [9], Sc [10] and Hf [11], have been used to decrease the optical damage of $LiNbO_3$. Especially, the effects Hf^{4+} ions in Fe:$LiNbO_3$ crystals were dissimilar to Mg^{2+} or Zn^{2+}. The HfO_2 doping concentration above its threshold value, the response rate and sensitivity are greatly improved. Meanwhile, the saturation diffraction efficiency remains at a high value.

In this paper, HfO_2 was the first time doped into Fe:Mn:$LiNbO_3$ crystals. Our purposes are to study the ions location in the host lattice and the nonvolatile holographic storage properties of Hf:Fe:Mn:$LiNbO_3$.

2. Experimental

2.1. Crystals growth and sample preparation

Hf:Fe:Mn:$LiNbO_3$ crystals were grown by Czochralski method in an air atmosphere. Various factors affecting the control of crystal growth and the relationship among these factors were analyzed, and an auto monitoring and adjusting diameter-constant control system was built up. Using this control system, various levels of HfO_2 doping crystals were successfully grown. These crystals show smooth surface from shoulder, body to tail. One of the crystals was shown in Fig. 1.

The crystals were placed in a furnace for polarizing at electric current intensity 5 mA/cm^2 for 30 min at 1200 °C and annealing for 8 h to room temperature. The crystals were cut into wafers with a dimension of 8 mm × 8 mm × 2.5 mm. All wafers were oxidized in Nb_2O_5 powders to be oxidized at 1100 °C for 18 h, as listed in Table 1.

2.2. Measurements

The OH^- infrared absorption peaks of the samples were measured by Fourier infrared spectrophotometer in the wavelength range of 3000–4000 cm^{-1} at room temperature.

The ultraviolet–visible optical absorption spectra of Hf:Fe:Mn:$LiNbO_3$ crystals were measured by a CARY1E UV–vis spectrophotometer. The measurement range was from 300 to 900 nm.

* Corresponding author. Tel.: +86 20 84113370; fax: +86 20 84115692.
E-mail addresses: wangbiao@mail.sysu.edu.cn, zzf0511@sina.com (B. Wang).

0030-4026/$ – see front matter © 2010 Elsevier GmbH. All rights reserved.
doi:10.1016/j.ijleo.2010.07.024

Table 1
The doped Hf:Fe:Mn:$LiNbO_3$ crystal samples in experiment.

Crystals	Composition	Dopant in starting melt
LN1	Fe:Mn:$LiNbO_3$	0.03 wt% Fe_2O_3, 0.1 wt% MnO_2
LN2	Hf:Fe:Mn:$LiNbO_3$	3 mol% HfO_2, 0.03 wt% Fe_2O_3, 0.1 wt% MnO_2
LN3	Hf:Fe:Mn:$LiNbO_3$	4 mol% HfO_2, 0.03 wt% Fe_2O_3, 0.1 wt% MnO_2
LN4	Hf:Fe:Mn:$LiNbO_3$	5 mol% HfO_2, 0.03 wt% Fe_2O_3, 0.1 wt% MnO_2

Fig. 1. The as-grown boule.

The optical damage resistance ability of the crystals was observed by straightly observing transmission facula distortion method. Fig. 2 shows the experimental setup. An argon-ion laser was used as light source, and the incident beam power level could be adjusted by an attenuator. The crystal *c*-axis was set parallel to the polarization direction of the laser beam and placed on the back focal plane of the convex lens. The power density of the beam spot passing through a pinhole on a light shield was measured by a photodiode connected with a computer. When the laser's power intensity achieves certain value, light scattering appears inside the crystal and the facula is elongated along *c*-axial of the crystal. The laser power intensity, which brings the distortion of the facula transited the crystal, is called the light-scattering ability resistance of the crystal.

The holographic properties were investigated by two waves mixing in transmission geometry at a fixed grating spacing (as shown in Fig. 3) at room temperature. In this experiment, these crystals were pre-exposed to the UV light (intensity, 40 mW/cm^2) for 1 h. Then two-color recordings were carried out in Hf:Fe:Mn:$LiNbO_3$ crystals at λ 532 nm together with the UV light. A Nd:YAG laser was split into two beams of equal intensity, with each being ~30 mW/cm^2. These two beams of extraordinary polarization were made to intersect symmetrically inside the crystal of 2.5 mm thickness so that the grating vector was parallel to the crystal *c*-axis. In the process of recording, one of the recording beams was blocked by a shutter from time to time, so that we could use the other recording beam to monitor the grating build-up process and to measure the diffraction efficiency η. Here η was defined as

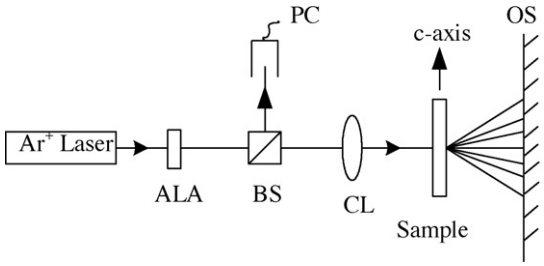

Fig. 2. Experimental setup of the light-scattering resistance ability. ALA: adjustable light attenuator, BS: beam splitter, PC: photocell, CL: convex lens, OS: observation screen.

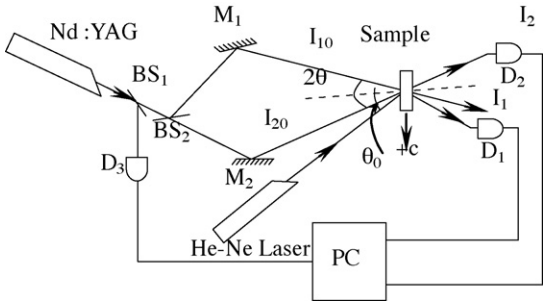

Fig. 3. Experimental setup of holographic storage. M_1, M_2: mirrors; BS_1, BS_2: beam splitters; D_1–D_3: detectors.

$I_d/(I_d + I_t)$, where I_d and I_t were the diffracted and transmitted intensities of the readout beam, respectively. A few percent of diffraction efficient could be achieved.

3. Results and discussion

3.1. Spectra analysis

The results are shown in Fig. 4. The OH^- absorption peak of LN1 is located at 3482 cm^{-1}, and the OH^- absorption peak of LN2 is at 3483 cm^{-1}. However, the OH^- absorption peaks of LN3 and LN4 crystals shift to 3489 cm^{-1}.The FWHM of absorption peaks of LN1and LN2 is wider than that of LN3 and LN4.

In congruent $LiNbO_3$, the ratio of Li to Nb is less than 1. The crystal is under the state of Nb-rich and Li-poor, so there are anti-site Nb defects $Nb_{Li}{}^{4+}$ and Li vacancy $V_{Li}{}^-$ defects in congruent $LiNbO_3$. In the case of the Fe:Mn:$LiNbO_3$, the doped Mn and Fe ions were located at Li^+ site in the formation of $Mn_{Li}{}^{+/2+}$ and $Fe_{Li}{}^{+/2+}$. When the doped concentration of Hf^{4+} ions in Fe:Mn:$LiNbO_3$ crystal was lower, Hf^{4+} replaced Nb $_{Li}{}^{4+}$. The OH^- absorption peaks will not change obviously. When the concentration of Hf^{4+} exceeded the threshold, a part of Hf^{4+} ions began to occupy Nb sites and existed in the form of $Hf_{Nb}{}^-$. Because $Hf_{Nb}{}^-$ has higher ability to attract H^+ than that of $V_{Li}{}^-$, which make the H^+ ions gather near the $Hf_{Nb}{}^-$. The mainly OH^- absorption peaks located at 3489 cm^{-1} described the vibration absorption situation of OH^- around $Hf_{Nb}{}^-$. High concentration of Hf^{4+} formed more $Hf_{Nb}{}^-$ defects, so the OH^- absorption peak becomes sharper.

We know that in Zn:Fe:$LiNbO_3$ crystals with its ZnO doping concentrations above threshold, besides 3529 cm^{-1} absorption peak related with $Zn_{Nb}{}^{3-}$–($V_{Li}{}^-$–OH^-) complex, another peak corresponding to the vibration of $Fe_{Nb}{}^{2-}$–($V_{Li}{}^-$–OH^-) appears at 3504 cm^{-1} [7]. It should be noted that 3504 cm^{-1} absorption peak is not present in LN3 and LN4, which suggests that most of Fe and Mn ions are unaltered their position and still located at Li sites.

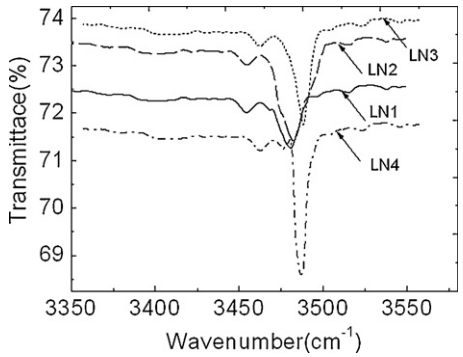

Fig. 4. The infrared absorption spectra of Hf:Fe:Mn:$LiNbO_3$ crystals.

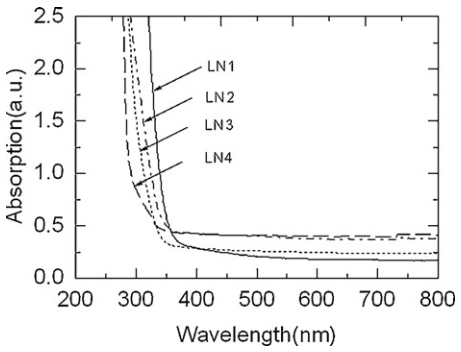

Fig. 5. UV absorption spectrum of Hf:Fe:Mn:$LiNbO_3$.

Fig. 5 shows the ultraviolet–visible absorption spectra of the Hf:Fe:Mn:$LiNbO_3$ crystals. It can be clearly seen that the absorption edges of LN2, LN3 and LN4 crystals successively shifted to the violet band, in comparison with that of the LN1.

The fundamental optical absorption edge is decided by valence electron transition energy from 2*p* orbits of O^{2-} to 4*d* orbits of Nb^{5+}. So the valence electronic state of O^{2-} directly affects the site of the absorption edge. In this paper, the phenomenon of the absorption-edge shift is explained by Z^{*2}/r, where $Z^* = Z - \Sigma s$; Z^*, Z, Σs, and r are the effective nuclear charge number, the atomic ordinal number of the ion, the shield factor, and the radius of the ion, respectively. The polarization ability of the ions was calculated by $Z^* = Z - \Sigma s$, where the value for Nb^{5+}, Fe^{3+}, Fe^{2+}, Mn^{3+}, Mn^{2+}, Hf^{4+}, and Li^+ are 52.5, 55.3, 42.2, 48.3,33.6, 44.6, and 2.5, respectively.

The interaction of positive and negative ions results in the change of the polarization ability of O^{2-}. If the polarization ability of the doping ion is lower than that of the replaced ion, which makes the polarization ability of O^{2-} decrease, the energy required by the electron transition increases. In this way the absorption-edge shifts to the violet band. We know that in the Fe:Mn:$LiNbO_3$ crystal, the Fe and Mn ions occupy the normal Li sites. When the HfO_2 doping concentration is below the threshold concentration, most of the Hf^{4+} ions replace the $Nb_{Li}{}^{4+}$ ions and form $Hf_{Li}{}^{3+}$. As the polarization ability of Hf^{4+} is lower than that of Nb^{5+}, the absorption edges of the LN2 shift to shorter wavelength compared with that of the LN1. When the doping concentration of HfO_2 is above the threshold concentration, all of the $Nb_{Li}{}^{4+}$ ions are replaced by a portion of the Hf^{4+} ions and the remaining Hf^{4+} begin to occupy normal Nb sites. As the polarization ability of Hf^{4+} is lower than that of Nb^{5+}, so the absorption-edge positions of the LN3 and LN4 successively shifted to the violet band.

3.2. The optical damage resistance ability

The results of the photo-damage-resistant ability of Hf:Fe:Mn:$LiNbO_3$ crystals are shown in Table 2. The results indicated that the photo-damage-resistant ability of LN3 and LN4 is about one order of magnitude higher than LN1.

According to the following well-known simplified Scalar expression, $\delta\Delta n \approx B\kappa\alpha I/\sigma$, where B is the generalized electro-optical coefficient, κ is the glass constant, α is the optical absorption coefficient, I is the intensity of the light and σ is the conductivity ($\sigma = \sigma_d + \sigma_p$, σ_d is the dark conductivity and σ_p is the photoconductivity, $\sigma_d \ll \sigma_p$, so $\sigma \approx \sigma_p$), the photorefractive ability of the

Table 2
The results of optical damage resistance ability (R) of the Hf:Fe:Mn:$LiNbO_3$ crystals.

Crystal	LN1	LN2	LN3	LN4
R (W/cm^2)	1.8×10^2	3.3×10^2	7.9×10^3	8.1×10^3

Table 3
Characteristic parameters of nonvolatile holographic storage in the oxidized Hf:Fe:Mn:$LiNbO_3$ crystals.

Crystals	Writing times (min)	Saturation diffraction efficiency (%)	Nonvolatile diffraction efficiency (%)
LN1	47	29.5	19.2
LN2	34	25.1	14.7
LN3	25	20.8	12.4
LN4	26	20.1	12.5

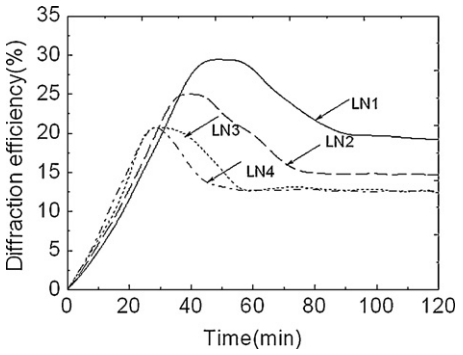

Fig. 6. The dependence of the diffraction efficiency on the time.

$LiNbO_3$ crystal increases with the decrease of the photoconductivity. From the analysis above, we know that when the HfO_2 doping concentration is below the threshold concentration, most of the Hf^{4+} replaces the $Nb_{Li}{}^{4+}$. The increasing photoconductivity, which is mainly attributed to the decrease of anti-site Nb_{Li}, induces the increase in photo-damage resistance ability. When the HfO_2 doping concentration is over the threshold concentration, most of the $Nb_{Li}{}^{4+}$ ions disappeared, so the photo-damage resistance ability will never increase.

3.3. Nonvolatile hologram storage properties

The results of holographic storage properties of Hf:Fe:Mn:$LiNbO_3$ are shown in Table 3. In Table 3, the response time of LN3 and LN4 is shorter than that of LN1 and LN2, though the diffraction efficiency has a little decrease. As it has been commented above, Fe^{3+} and Mn^{3+} ions also remain at Li sites in LN3 and LN4 acting as electron acceptors, therefore, the nonvolatile saturation diffraction efficiency of LN3 and LN4 crystal do not greatly decrease with respect to that of LN2 (Fig. 6).

4. Conclusion

In this paper, a series of Hf:Fe:Mn:$LiNbO_3$ crystals were prepared by Czochralski method. We studied the behavior of OH^- absorption peak, fundamental absorption edge, and optical damage as a function of HfO_2 doping concentration. Hf^{4+} takes priority in replacing anti-site Nb in Hf:Fe:Mn:$LiNbO_3$ crystals, when the concentration of HfO_2 exceeds its threshold value, and Hf^{4+} replaces Nb^{5+}, forming $Hf^{4-}{}_{Nb}$. Few of Fe and Mn ions are repelled to Nb^{5+} sites by Hf^{4+}. The optical damage resistance of Hf:Fe:Mn:$LiNbO_3$ increases rapidly when the concentration of HfO_2 exceeds the threshold value. The nonvolatile two-color holographic recording experimental results showed that the recording speed was faster with the increase of HfO_2 doping concentration, especially in LN3 and LN4, which exceeded the so-called threshold concentration, and at the same time little loss of nonvolatile diffraction efficiencies could be achieved.

Acknowledgements

This work was supported by the National Natural Science Foundation of China (10732100).

References

[1] D.L. Staebler, W.J. Burke, W. Philips, J.J. Amodei, Multiple storage and erasure of fixed holograms in Fe-doped $LiNbO_3$, Appl. Phys. Lett. 26 (1975) 182–184.
[2] F.H. Mok, Angle-multiplexed storage of 5000 holograms in lithium niobate, Opt. Lett. 18 (1993) 915–917.
[3] K. Buse, A. Adibi, D. Psaltis, Non-volatile holographic storage in doubly doped lithium niobate crystals, Nature 393 (1998) 665.
[4] Y. Liu, L. Liu, Ch. Zhou, Nonvolatile photorefractive holograms in $LiNbO_3$:Cu:Ce crystals, Opt. Lett. 25 (2000) 908–910.
[5] Y. Furukawa, M. Sato, F. Nitanda, K. Ito, Optical damage resistance and crystal quality of $LiNbO_3$ single crystals with various [Li]/[Nb] ratios, J. Cryst. Growth 99 (1990) 832.
[6] G.Q. Zhang, G.Y. Zhang, S.M. Liu, J.J. Xu, Q. Sun, The threshold effect of incident light intensity for the photorefractive light-induced scattering in $LiNbO_3$:Fe,M ($M = Mg^{2+}$, Zn^{2+}, In^{3+}) crystals, J. Appl. Phys. 83 (1998) 4392.
[7] T.R. Volk, V.I. Pryalkin, N.M. Rubinina, Optical damage resistant $LiNbO_3$–Zn crystal, Opt. Lett. 15 (1990) 996.
[8] J. Zhong, J. Jin, Z. Wu, Measurement of optically induced refractive-index damage of lithium niobate doped with different concentration of MgO, in: 11th International Quantum Electronics Conference, New York, 1980, pp. 631–635 (IEEE Catalog. No. 80, CH 1561-0).
[9] Y.F. Kong, J.K. Wen, H.F. Wang, New doped lithium-niobate crystal with high-resistance to photorefraction $LiNbO_3$:In, Appl. Phys. Lett. 66 (1995) 280.
[10] J.K. Yamanoto, K. Kitamura, N. Iyi, S. Kimura, Y. Furukawa, M. Sato, Increased optical-damage resistance in Sc_2O_3-doped $LiNbO_3$, Appl. Phys. Lett. 61 (1992) 2156.
[11] S. Li, S. Liu, Y. Kong, J. Xu, G. Zhang, Enhanced photorefractive properties of $LiNbO_3$:Fe crystals by HfO_2 codoping, Appl. Phys. Lett. 89 (2006) 101126.